ARTICLE IN PRESS

Available online at www.sciencedirect.com

ScienceDirect

International Journal of Rock Mechanics & Mining Sciences ▮ (▮▮▮▮) ▮▮▮–▮▮▮

International Journal of Rock Mechanics and Mining Sciences

www.elsevier.com/locate/ijrmms

On drawbody shapes: From Bergmark–Roos to kinematic models

F. Melo[a,*], F. Vivanco[a], C. Fuentes[b], V. Apablaza[b]

[a]*Departamento de Física Universidad de Santiago de Chile and Center for Interdisciplinary Research in Materials, CIMAT Avenida Ecuador 3493, Casilla 307 Correo 2 Santiago, Chile*

[b]*Instituto de Innovación en Minería y Metalurgía, IM2 Codelco Avenida del Valle 738, Ciudad Empresarial, Huechuraba, Santiago, Chile*

Accepted 24 April 2006

Abstract

The geometrical locus defined by the initial location of the fragments that are recovered from an extraction point in underground mining, after a given operation, is commonly named ''drawbody''. A brief review of drawbody shapes in flat-bottomed hoppers is proposed. The Bergmark–Roos hypothesis is discussed and it is shown that when the continuity equation is considered, particle density increases with time and when moving toward the hopper aperture. Drawbody shapes are calculated for flows predicted from a plasticity approach, as well as from a kinematic model. Applications to complex configurations in which the flow is produced by two drawpoints, either in simultaneous or sequential extractions, are discussed in some detail. In particular, the extracted zone is calculated exactly and its dependence on distance between drawpoints is investigated. The knowledge of such locus should prove valuable when optimizing ore recovery in mining processes.

PACS: 5.70.Mg; 45.70.Vn; 47.57.Gc

Keywords: Block caving; Isolated extracted zone; Drawpoints, Kinematic flow model

1. Introduction

The relatively poor understanding of granular flows and ore extraction from a caving rock mass is currently an area of concern in industry and research. The importance of gravity flows, the related open problems as well as the approaches available for mining applications have been recently discussed by several authors, for instance Brown [1] and Rustan, [2]. As pointed out by these authors, the lack of analytical formulations to account for the relevant parameters involved in optimizing ore recovery implies a high degree of reliance on computer modeling. However, most of the computational models available to describe industrial granular flows are not necessarily based on the first principles of mechanics and therefore cannot be qualified by reference to canonical verification problems. Most experimental efforts have been focused on the prediction of the initial locus of the material that is extracted from a single aperture. Such a locus is named the ''drawbody'' or isolated extracted zone (IEZ) and depends mainly on the volume of the extracted material. However, little progress has been achieved in predicting the IEZ from first principles. To date, the mathematical equation that best describes the shape of the extraction drawbody is the Bergmark–Roos equation (see Refs. [3,4] for a recent review). In addition, due to the lack of both analytical models and reliable experimental data, the flow resulting from interactions of several drawpoints is completely unknown. Thus, in this complex situation, the locus of extracted material is roughly estimated by the elementary geometrical superposition of IEZs produced by the drawpoints under study. A precise knowledge of the extracted zone in complex combinations of drawpoints is however crucial to optimize ore recovery in underground mining when applying the well-known ''block caving method'' [1]. A sketch of the common geometry used in block caving is presented in Fig. 1. In this method, a large

*Corresponding author.
E-mail address: fmelo@lauca.usach.cl (F. Melo).

1365-1609/$ - see front matter © 2006 Published by Elsevier Ltd.
doi:10.1016/j.ijrmms.2006.04.010

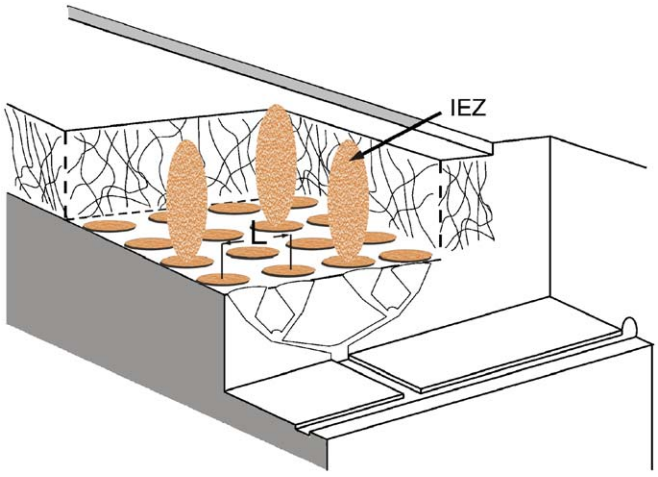

Fig. 1. Schematic distribution of drawpoints employed in the block caving method. Vertical and horizontal cuts intend to show the main geometrical features of the hoppers used in underground mining. The roughly ellipsoidal shapes on top of several hoppers mimic the IEZs.

number of hoppers are organized in a periodic lattice in which the geometry and distance between neighbors intend to optimize the global extraction process. Besides the size of hopper apertures and the distance between hoppers, an important parameter is the average size of granulates which might strongly influence the average size of the IEZ. In turn, the geometry of the IEZ tells us to what extent any two neighboring IEZs might interact.

In the present article, we first briefly discuss the hypothesis made for the determination of IEZ in the Bergmark–Roos formulation. We show that the velocity field used in the original derivation leads to an important density increase as the fragments approach the hopper aperture. This effect is the source of the relatively elongated shape of the drawbody in the Bergmark–Roos approximation. To check the sensitivity of these results on the particular choice of the form of the flow, we calculate the isolated "drawbody" for velocity fields derived from plasticity theory for granular materials [5]. We show that, with this approximation, the drawbody is rather insensitive to the particular choice of the angular dependence of the flow. However, radial dependence, which insures constant mass density, is more critical since it produces "drawbody" shapes that are lower and therefore wider than the ones predicted by the Bergmark–Roos approximation. In the last section, we apply the kinematic model to calculate "streamlines" and isolated "drawbodies" for several simple configurations. We exploit as well the linearity of the kinematic model to provide insight into flows and extracted zones produced by the simultaneous contribution of two drawpoints. We finally use the plasticity model to illustrate the form of an extracted zone resulting from sequential extraction occurring at two neighboring drawpoints. A brief discussion is proposed in the concluding section on possible strategies to calculate complex streamlines and shapes of extracted zones by the use of the superposition principle.

2. Bergmark–Roos review

As stated in Ref. [2], it is well accepted that the Bergmark–Roos theory, which was a paradigm shift in the science of gravity flow, is today probably the best mathematical theory for calculating the drawbody for a homogeneous material or when we wish to estimate the mean drawbody shape for a large number of draws. To better understand the physical basis on which this theory is sustained we present, in this section, a brief review of the underlying analysis leading to Bergmark–Roos drawbody shape.

The main hypothesis employed during the development of the Bergmark–Roos formulation, as discussed in Ref. [4], is that fragments move in straight lines from their resting point to the opening where they are removed continuously. Another important assumption of the model is that the fragments are influenced solely by two opposite forces, namely the gravitational force and the friction force due to the interaction with the surrounding fragments. Defining the angular coordinate θ, with respect to the vertical, the gravity force is $-mg\cos\theta$, with m being the mass of a fragment and g the gravity acceleration.

In the Bergmark–Roos derivation, it is also assumed that the acceleration of a single granulate is constant during the entire movement. From the force balance, the acceleration reads, $a_r(\theta) = g(\cos\theta - \cos\theta_G)$, for $|\theta| \leqslant \theta_G$, where θ_G is the maximum allowed angle for displacement i.e., the angle at which the friction force equals particle weight, $mg\cos\theta_G = F_f$, with F_f being the friction force [4]. With our definitions, the aperture has a width $2D = 2r_D\sin\theta_G$ and is located at a distance r_D from the origin of the polar coordinates, as indicated in Fig. 2. Notice that with this choice of coordinates, the acceleration is negative, thus $a_r(\theta) = |-g(\cos\theta - \cos\theta_G)|$.

In addition, in this approximation, initially all the particles are assumed to be at rest. Thus, the velocity field is, $V_r = -a_r(\theta)t$ and $V_\theta = 0$. By integrating the radial speed in time, the radial location of particles reads, $r(\theta,t) = r_0(\theta) - \frac{1}{2}a_r(\theta)t^2$, where $r_0(\theta) = r(\theta, t=0)$ is the initial location of the particles that are found at position

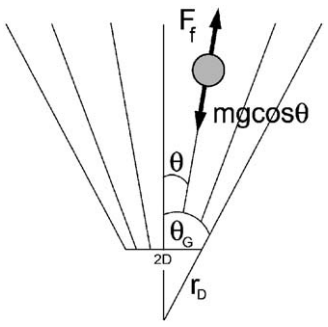

Fig. 2. Schema of the polar coordinate system and drawpoint parameters used here for the Bergmark–Roos derivation of IEZ. Angles are measured from the vertical and with this choice of the origin the aperture locates at a distance r_D.

$r(\theta,t)$ after a time t. Thus, the drawbody, defined as the initial location of the particles that cross the aperture at a given time t, $r(\theta,t)=r_D$, is given as, $r_0(\theta,t)=r_D+\frac{1}{2}a_r(\theta)t^2$, which, in terms of its maximum height, $r_{\max}$, occurring at $\theta=0$, reads,

$$r_0(\theta,r_{\max})-r_D=(r_{\max}-r_D)\frac{\cos\theta-\cos\theta_G}{1-\cos\theta_G}, \tag{1}$$

where $r_{\max}=r_D+(gt^2/2)(1-\cos\theta_G)$.

We now verify to what extent the velocity field in Eulerian coordinates derived from Bergmark–Roos assumptions respects local mass conservation. For simplicity, we first analyze the two-dimensional case in which the continuity equation reads

$$\frac{\partial\rho}{\partial t}+\frac{1}{r}\frac{\partial(r\rho V_r)}{\partial r}=0, \tag{2}$$

where ρ is the local material density. Notice that ρ must be a function of space and time, otherwise, the continuity equation is not obeyed. The general solution is, $\rho(r,t)=f(r+a_r(\theta)t^2/2)/r$, where f is a function to be determined by the initial density of the material. If the density is initially constant, $\rho=\rho_i$, then $f=\rho_i r$ in $t=0$. The general evolution of such homogeneous density is thus, $\rho=\rho_i(1+a_r(\theta)t^2/2r)$, which can be written simply as, $\rho=\rho_i r_{0r}/r$, where r_{0r} is the position at $t=0$ of the particle located at position r at time t. Thus, if particles do not move, no density variation occurs. However, a volume element traveling down experiences a density increase that is a function of its path length.

To check the consistency of the results presented above, the total section S_0 of the drawbody can be calculated by integrating the mass flow passing through the aperture as follows:

$$S_0=-\int_{-\theta_G}^{\theta_G}\int_0^t\frac{\rho(r_D,t')}{\rho_i}V_r r_D\,\mathrm{d}\theta\,\mathrm{d}t', \tag{3}$$

which can be written,

$$S_0=\int_{-\theta_G}^{\theta_G}\int_0^t r_0(\theta,t')a(\theta)t'\,\mathrm{d}\theta\,\mathrm{d}t'=\int_{-\theta_G}^{\theta_G}\int_0^t\frac{1}{2}\frac{\mathrm{d}r_0^2(\theta,t')}{\mathrm{d}t'}\,\mathrm{d}\theta\,\mathrm{d}t'. \tag{4}$$

Once integrated in time, the latter becomes the known formula for the drawbody section

$$S_0=\int_{-\theta_G}^{\theta_G}\frac{1}{2}(r_0^2(\theta,t)-r_D^2)\,\mathrm{d}\theta, \tag{5}$$

which can be integrated to express the $r_{\max}$ in terms of S_0. This is,

$$S_0=\left(\frac{r_{\max}-r_D}{1-\cos\theta_G}\right)\{2r_D(\sin\theta_G-\theta_G\cos\theta_G)-\left(\frac{r_{\max}-r_D}{1-\cos\theta_G}\right)(3\sin\theta_G\cos\theta_G-2\theta_G\cos^2\theta_G-\theta_G)\}. \tag{6}$$

The same analysis can be carried out in the three-dimensional configuration. The respective continuity equation reads

$$\frac{\partial\rho}{\partial t}+\frac{1}{r^2}\frac{\partial(r^2\rho V_r)}{\partial r}=0, \tag{7}$$

whose solution is $\rho(r,t)=f(r+a_r(\theta)t^2/2)/r^2$. Here, f is a function to be determined from the initial density of the material. Thus, if the density is initially constant, $\rho=\rho_i$, then $f=\rho_i r^2$ at $t=0$. The general evolution of such homogeneous density is then, $\rho=(\rho_i/r^2)(r+a_r(\theta)t^2/2)^2$. Again, as in the two-dimensional case, an curious increase of density of the material occurs as time progresses.

To complete our discussion, we derive the drawbody shape as a function of its height, $r_{\max}=r_D+(gt^2/2)(1-\cos\theta_G)$, and a finite hopper aperture of radius $r_D\sin\theta_G$. As before, the aperture is located at a distance r_D from the origin of the spherical coordinates. Expressing the time dependence as a function of angular and radial variables, we obtain,

$$r_0(\theta,r_{\max})-r_D=(r_{\max}-r_D)\frac{\cos\theta-\cos\theta_G}{1-\cos\theta_G}. \tag{8}$$

After a calculation similar to the one of the drawbody section in two dimensions, the drawbody volume Ω_0 reads

$$\Omega_0=\frac{\pi}{6}(1-\cos\theta_G)[r_{\max}^3-3r_D^3+r_{\max}^2r_D+r_{\max}r_D^2], \tag{9}$$

which, in the limit of $r_{\max}\gg r_D$, becomes

$$\Omega_0=\frac{\pi}{6}r_{\max}^3(1-\cos\theta_G). \tag{10}$$

This is the Bergmark–Roos formula for an isolated drawbody [4], expressed in terms of the angular variables used here. Notice that, to calculate the drawbody shape as a function of the extracted volume Ω_0 and the hopper aperture r_D, the third order algebraic Eq. (9) must be solved. This allows one to obtain $r_{\max}$ expressed in terms of the desired variables. The appropriate solution, although algebraically complex, can be found easily.

In summary, the analysis presented above shows that the Bergmark–Roos theory for drawbody is unphysical since it involves a strong density increase as the granular material approaches the hopper aperture. However, it is not surprising that, in many cases, this theory predicts the approximate observed shapes of the drawbody, since mass is globally conserved through the volume of interest. To further investigate this last point, in the following, we calculate drawbody shapes deduced from plasticity models for granulate flows and we show that these shapes have the same general features than that obtained from Bergmark–Roos prediction.

3. Plasticity theory for granular flows

In general, flows in granular materials are described by hydrodynamical type of models whenever the characteristic size of the container is much larger than the particle size,

since under this condition it is expected that velocity and force fluctuations would be much smaller than the average values. The commonest coarse grained approach for the predictions of velocity distribution in granular materials is based on plasticity theory. In these models, that are described in detail in Ref. [5], the stress distribution in the static material is first calculated and from this the velocity distribution is obtained. Although, little progress has been achieved for the prediction of velocity fields in specific cases, plasticity theory provides more realistic predictions for granular flows in hoppers. Thus, we consider it interesting to derive the shape of the drawbody for such fields. In three-dimensional flows, the azimuthal and radial field are not known precisely as they are functions of geometrical variables and particle features. However, in gravity flows for axis symmetric situations, it is a good approximation to consider that the azimuthal velocity vanishes [5]. To insure incompressibility, a $1/r^2$ dependence must be included for the radial velocity, which is written as

$$V_r = \frac{-V_0 r_D^2}{r^2} f(\theta, \phi), \tag{11}$$

where θ is the angular coordinate measured from the vertical, r_D is the radial position of the aperture of radius $r_D \sin\phi$ and V_0 is the speed at the middle of the aperture. For conical hoppers, $\phi = \theta_W$ and $f(\theta, \phi)$ is selected to respect the boundary conditions imposed at the hopper lateral walls which are, in turn, functions of wall friction. Although for flat-bottomed hoppers the radial approximation is less clear, we will use it here only to make comparison with the flow introduced in the previous section. Thus, for flat-bottomed hoppers ϕ should be equal to θ_G and f must vanish at the sliding internal angle θ_G, i.e., $f(\theta = \theta_G) = 0$. Experimentally, it has been shown in a variety of hoppers that the two-dimensional flow can be represented by a radial velocity field as, $V_r = (-V_0 r_D/r)\cos\pi\theta/2\theta_G$. As a generalization of these results, let us first consider, $f(\theta, \theta_G) = \cos\pi\theta/2\theta_G$, vanishing at $\theta = \pm\theta_G$, for the three-dimensional case. Then, the radial speed can be expressed as

$$V_r = \frac{-V_0 r_D^2}{r^2} \cos\frac{\pi\theta}{2\theta_G}. \tag{12}$$

Writing $dr/dt = V_r$, the particle trajectories are obtained and, with them, the drawbody reads

$$\frac{r_0^3(\theta) - r_D^3}{r_{\max}^3 - r_D^3} = \cos\frac{\pi\theta}{2\theta_G}, \tag{13}$$

where $r_{\max}$ is the drawbody height located at $\theta = 0$. $r_{\max}$ can be related to the total extracted volume as follows:

$$\Omega_0 = \frac{2\pi}{3}\left(\frac{r_{\max}^3 - r_D^3}{(\pi/2\theta_G)^2 - 1}\right)\left(\frac{\pi}{2\theta_G}\sin\theta_G - 1\right). \tag{14}$$

The drawbody shape obtained from Eq. (13) is represented in Fig. 3. Before going into detailed comparisons, let us assume the same angular dependence of the radial speed as

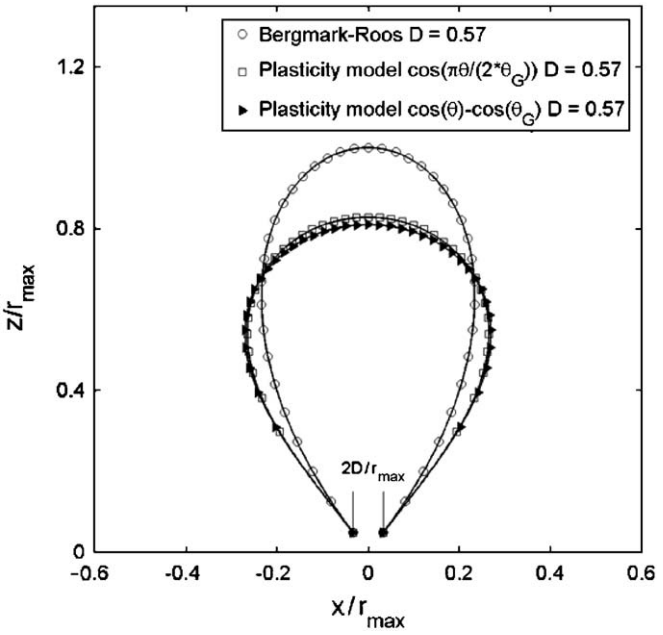

Fig. 3. Drawbody for the Bergmark–Roos theory Eq. (8) in contrast to the one obtained from the plasticity model from Eqs. (13) and (17) for equal volume. Here, $\theta_G = 35^\circ$, $r_D = 1$, $r_{\max} = 17$. Notice that $r_{\max}$ here refers to Bergmark–Roos and all distances are in arbitrary units of length.

that introduced by Bergmark–Ross. Thus, $f(\theta, \phi = \theta_G) = \cos\theta - \cos\theta_G$ and the radial field now reads

$$V_r = \frac{-V_0 r_D^2}{r^2}(\cos\theta - \cos\theta_G). \tag{15}$$

With this choice, the streamlines remain radial and particle trajectories are described by

$$r_0(\theta)^3 - r_D^3 = 3r_D^2 V_0 t(\cos\theta - \cos\theta_G). \tag{16}$$

Writing the time t as a function of $r_{\max}$, the drawbody shape becomes

$$\frac{r_0^3(\theta) - r_D^3}{r_{\max}^3 - r_D^3} = \frac{\cos\theta - \cos\theta_G}{1 - \cos\theta_G}, \tag{17}$$

where $r_{\max}^3 = r_D^3 + 3r_D^2 V_0 t(1 - \cos\theta_G)$ is obtained from the total mass conservation, i.e., the drawbody volume equals the total extracted material to date t

$$\Omega_0 = \frac{\pi}{3}[r_{\max}^3 - r_D^3]\frac{\cos^2\theta_G - 2\cos\theta_G + 1}{(1 - \cos\theta_G)}. \tag{18}$$

In Fig. 3 the drawbody shape predicted by the Bergmark–Roos approximation is contrasted to the ones obtained from plasticity models Eqs. (13) and (17). First, it is seen that the drawbody shape predicted by plasticity models is rather insensitive to the form of the function $f(\theta)$ selected. The value of θ_G is, however, more critical as relatively little variation in this quantity produces notable changes in $r_{\max}$. Thus, in all cases, care must be taken to determine the suitable value of θ_G. Secondly, the Bergmark–Roos drawbody is notably taller than that predicted by plasticity flows. This is because the Bergmark–Roos flow does not

respect incompressibility, since it was shown in a previous section that the material density increases toward the hopper aperture as time progresses. In other words, the resulting radial speed of fragments is overestimated in regions where their effective acceleration is large. Thus, for a given time, particles located at comparatively larger distances along the vertical can reach the aperture, giving rise to more elongated shapes.

4. Kinematic model

In the present section, we first comment on a few aspects of the kinematic model that are important to establish the validity of the drawbody shapes we derive.

In early works, Mullins [6] proposes an alternative approach to the predictions of velocity distributions by modeling the flow as the upward diffusion of voids by random processes. The validity of this model, better known as diffusive, is not obvious since it is not derived from force balance equations. Similar ideas are developed by Litwiniszyn [7], who considers that the particles are confined to a series of hypothetical cages. When a particle falls out of a cage, it can be replaced by those particles located just above, with equal probability. Thus, the probability P, of a particle being in motion, is given by the solution of a diffusion equation, $\partial_y P = D_P \partial_{xx} P$. D_P is a diffusion coefficient which is proportional to particle diameter d, $D_P \sim d/8$. As shown in [7], P is proportional to the particle displacements which, provided they are not too large, will be related to the vertical velocity v. This last assumption is, however, a subject of debate. To overcome this difficulty, Nedderman and Tüzün [8] developed a model in which the particles immediately above the orifice fall out of the hopper and the particles above the layer slide into the vacant space. Similarly, the next layer slips into the newly created space. For this process, it is assumed that the weight of each particle is enough to cause the motion which is unaffected by any stress in the system, hence this model is purely kinematic. Basically, if two particles in the lower layer have different velocities, there will be a tendency for the particle just above to move laterally in the direction of the fastest falling particle. Thus, it is expected that $U = -D_p \partial_x V$, where U and V are the horizontal and vertical velocities, respectively. Using mass conservation, it is easy to find, $\partial_y V = D_P \partial_{xx} V$. The same authors have shown that the kinematic model is very successful to describe velocity distribution in rectangular hoppers under stationary conditions and when the material is not compact [8]. Recent works [9,10] have confirmed these findings showing that the streamlines are correctly predicted by kinematic models for loose packing preparations. However, when the material in the hopper is in a nearly compact state, the agreement becomes poor [11], since when a densely packed material begins to flow, dilation takes place in the vicinity of the initial failure surface; a front of dilation propagates upwards producing cumulative errors in the fragmentdisplacement [12]. Naturally, these deviations increase with height. A last remark is that the kinematic description developed in [8] does not include dynamic considerations, hence it requires precise knowledge of the speed distribution at the hopper aperture. This is the kind of information that can only be provided by a real dynamic analysis or detailed experimental observations. In addition, shear bands found in particular configurations of silos and hoppers are reminiscent of a solid–liquid transition-like behavior and cannot be captured by this kind of approach [5]. Thus, in this section we only consider flows in flat-bottomed hoppers containing granular material that is loosely packed.

In the three-dimensional configuration, the kinematic model hypothesizes [8]

$$V_x = -D_P \frac{\partial V_z}{\partial x} \tag{19}$$

and

$$V_y = -D_P \frac{\partial V_z}{\partial y}. \tag{20}$$

From the condition of constant density, which is,

$$\frac{\partial V_x}{\partial x} + \frac{\partial V_y}{\partial y} + \frac{\partial V_z}{\partial z} = 0, \tag{21}$$

the equation for the vertical velocity becomes

$$\frac{\partial V_z}{\partial z} = D_P \left[\frac{\partial^2 V_x}{\partial x^2} + \frac{\partial^2 V_y}{\partial y^2} \right]. \tag{22}$$

4.1. Streamlines and drawbody in two dimensions for narrow aperture

The aim of this subsection is to determine the exact shape of the drawbody as well as the streamlines, in the workframe of the kinematic model for the simplest configuration. In two-dimensional flows, the streamlines obey the following equation:

$$\frac{dx}{V_x} = \frac{dy}{V_y}, \tag{23}$$

where the y-axis is oriented along the vertical. The kinematic model reduces to $\partial V_y/\partial y = D_P \partial^2 V_y/\partial x^2$ and $V_x = -D_P \partial V_y/\partial x$ in two dimensions, which in the case of an infinitely narrow aperture accept as solution:

$$V_y = \frac{-Q}{\sqrt{4\pi D_P y}} \exp\left(-\frac{x^2}{4 D_P y}\right),$$
$$V_x = \frac{-Q}{\sqrt{4\pi D_P y}} \exp\left(-\frac{x^2}{4 D_P y}\right) \frac{x}{2y}, \tag{24}$$

where Q is the sectional flow rate, i.e., section of extracted granular material per unit of time. Thus, the equation for streamlines reads

$$\frac{dx}{dy} = \frac{x}{2y}, \tag{25}$$

whose solution is given by

$$y = cx^2, \tag{26}$$

where c is a constant along a given streamline. At this point we note that streamlines have been measured accurately by Caram and Hong [9] in a quasi-two-dimensional configuration and excellent agreement has been obtained for the diffusive model.

Following our program to calculate the drawbody zone, it is first necessary to find the particles pathlines. Since a particle under consideration is moving with the fluid at its local velocity, pathlines must satisfy the equations

$$\frac{\mathrm{d}x}{\mathrm{d}t} = \frac{-Q}{\sqrt{4\pi D_P y}}\exp\left(-\frac{x^2}{4D_P y}\right)\frac{x}{2y},$$
$$\frac{\mathrm{d}y}{\mathrm{d}t} = \frac{-Q}{\sqrt{4\pi D_P y}}\exp\left(-\frac{x^2}{4D_P y}\right). \tag{27}$$

Using the streamline solution and integrating one of the above equations, we find

$$\frac{4\sqrt{\pi c^3 D_P}}{3}(x_0^3 - x^3)\exp\left(\frac{1}{4cD_P}\right) = Qt \tag{28}$$

or equivalently,

$$\frac{4\sqrt{\pi D_P}}{3}(y_0^{3/2} - y^{3/2})\exp\left(\frac{1}{4cD_P}\right) = Qt, \tag{29}$$

where x_0 and y_0 are the coordinates of a particle at $t = 0$. Remembering that c is a constant that labels all the streamlines, the above equations allow following all particle trajectories as a function of time.

Now, the drawbody is just the location at $t = 0$ of the particles that, at a given time t, cross the aperture, which is,

$$\frac{4}{3}\sqrt{\pi D_P}\exp\left(\frac{x_0^2}{4D_P y_0}\right)y_0^{3/2} = Qt, \tag{30}$$

which allows calculating the drawbody $y_0 = y_0(x_0, t)$ for a given time t, at the extraction rate Q. The drawbody shape can be calculated numerically without difficulty. Let us now calculate analytically its maximum height $y_0^{\max}$ and its maximum width, $w_0^{\max} = x_0^+ - x_0^-$ occurring at $y = y_0^*$, where $x_0^\pm$ are the coordinates of the points defining the largest horizontal distance of the drawbody. The maximum height is located at $x_0 = 0$ and reads

$$y_0^{\max} = \left(\frac{3Qt}{2\sqrt{4\pi D_P}}\right)^{2/3}. \tag{31}$$

The maximum width is obtained from the condition, $\mathrm{d}x_0/\mathrm{d}y_0|_{y_0^*} = 0$, which produces

$$\frac{x_0^{\pm 2}}{y_0^*} = 6D_P, \tag{32}$$

where y_0^* is given by, $y_0^* = (1/e)(3Qt/2\sqrt{4\pi D_P})^{2/3}$.

Since the calculations above are performed for an infinitely narrow hopper aperture, the drawbody shape obtained is valid when its width is large compared to the aperture size.

4.2. Drawbodies in three dimensions: infinitely small symmetric apertures

A similar calculation to the above can be performed for the three-dimensional case by just remembering that the velocity field is the solution to the diffusion equation (22), which in the case of cylindrical symmetry, reads,

$$\frac{\partial V_z}{\partial z} = D_P\left[\frac{1}{r}\frac{\partial}{\partial r}\left(r\frac{\partial V_z}{\partial r}\right)\right]. \tag{33}$$

In the case of a small circular aperture, it accepts as a solution

$$V_z = \frac{-Q}{4\pi D_P z}\exp\left(-\frac{r^2}{4D_P z}\right), \tag{34}$$

where we have used polar coordinates (r, θ) in the plane (x, y) and z as the vertical axis. The streamlines are easily calculated and, as before, we find parabolic shapes, $z = cr^2$. With this, the form of the drawbody is given implicitly by

$$2\pi D_P \exp\left(\frac{r_0^2}{4D_P z_0}\right)z_0^2 = Qt, \tag{35}$$

which allows calculating $z_0 = z_0(r_0, t)$ as a function of time t and the extraction rate Q (Fig. 4). Notice that here Q is a volumetric flow rate. We now calculate the drawbody maximum height $z_0^{\max}$, and its maximum width, $w_0^{\max} = 2r_0^{\max}$. The maximum height located at $r_0 = 0$ reads

$$z_0^{\max} = \left(\frac{Qt}{2\pi D_P}\right)^{1/2}. \tag{36}$$

As before, the maximum width is obtained from the condition, $\mathrm{d}r_0/\mathrm{d}x_0|_{z_0^*} = 0$, which produces

$$\frac{r_0^{\max 2}}{z_0^*} = 8D_P, \tag{37}$$

where z_0^* is given as $z_0^* = (1/e)(Qt/2\pi D_P)^{1/2}$.

4.3. Drawbodies in three dimensions: finite size apertures

The case of a finite size aperture is of major interest for more realistic applications. Unfortunately, the solution for the streamlines cannot be found in a compact formula, hence we solve it here numerically. The general form for the vertical velocity distribution in this case can be found in Chapter 8, p. 250 in Ref. [5], therefore, we do not repeat it here. The notation is equal to that used in [5], the orifice radius is b and the box size is a, except that the diffusion coefficient here is named D_P. Streamlines can be found [5] by numerically integrating the speed with a fourth order Runge–Kutta method. Fig. 5 illustrates the results for the extraction zone for several maximum heights of the drawbody. The effect of the orifice size is clearly observed and the drawbody width, in this case, is given approximatively by $w^0 \approx 2(b + \sqrt{D_P z_0^{\max}})$.

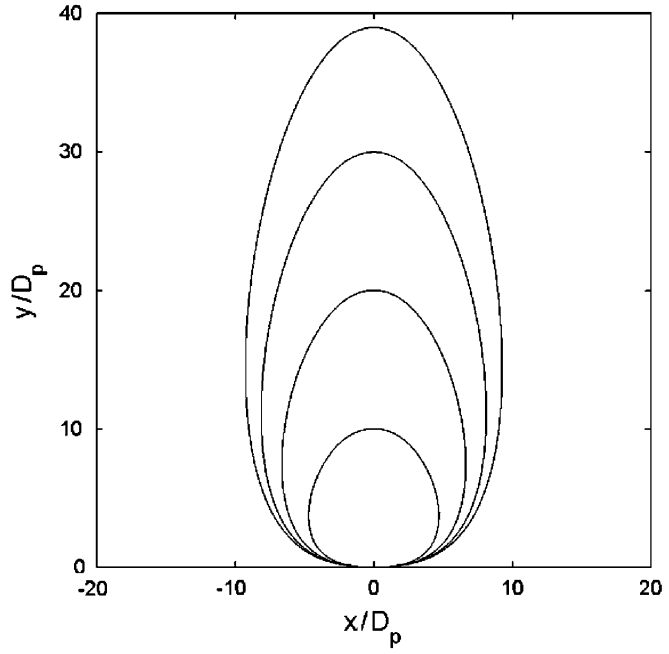

Fig. 4. Solid lines represent the drawbodies calculated from Eq. (35) as a function of the total amount of extracted material, $Qt = 75, 210, 390, 580$ expressed in units of D_P^2, where $D_P = 1$, in arbitrary units of length.

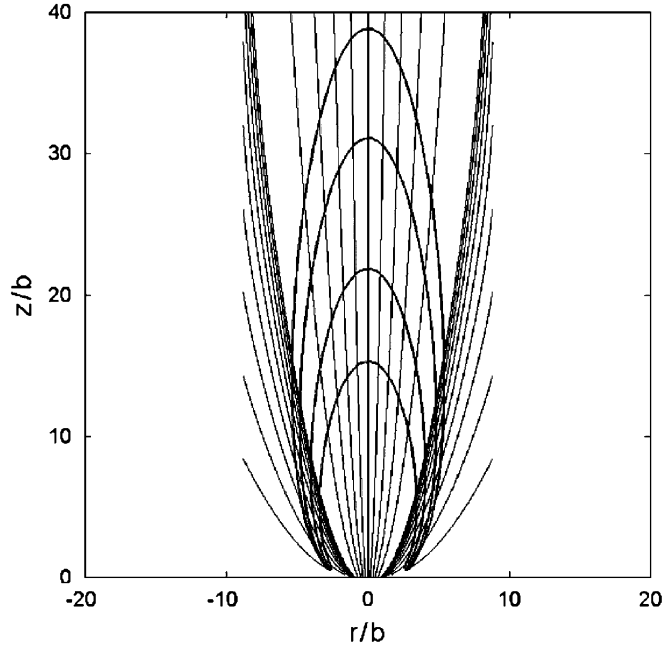

Fig. 5. The drawbody and the streamlines for an isolated aperture in three dimensions. Parameters are: the diffusion coefficient $D_P = 0.5$, the aperture radius $b = 2$, the box size $a = 20b$ and the maximum height of the drawbody $z_0^{\max}/b = 15, 22, 31, 39$. All these quantities are given in arbitrary units of length.

5. Extracted zone for several apertures: general case

We discuss below the total flow produced by the interaction of two apertures located some distance apart. Two important situations are distinguished depending on the selected strategy to carry out mineral extraction. In some cases, for instance in a continuous extraction process, it is useful to know the shape of the extracted zone when the flow takes place in both apertures simultaneously. However, more often the extraction only occurs first at a single aperture and then at its nearest neighbor. Naturally, there is a variety of possible combinations of these processes that, fortunately, can be easily generalized with the results described below.

5.1. Extracted zone for two apertures in simultaneous extraction

To illustrate the first case, we place ourselves on the workframe of the kinetic model and we take advantage of the fact that the velocity field obeys a linear partial differential equation. The linearity of this model simply implies that a linear combination of the linear equation solutions is a solution as well. Thus, in this model, the flow due to several apertures is quite straightforward as it corresponds to the superposition of the flow produced by each single aperture. In general this is written as

$$\vec{v} = \sum_{\vec{L}_i} \vec{v}_{Q_{0i}}(\vec{x} - \vec{L}_i), \tag{38}$$

where $\vec{v}_{Q_{0i}}$ is the velocity field produced by a single aperture with total flow rate Q_{0i} at the hopper aperture i, which is centered at position L_i. For mining application this result appears to be very useful since it is enough to characterize the flow produced by a single aperture to construct the flow of hoppers of multiple apertures. Naturally, care must be taken to correctly handle the boundary conditions imposed at the hopper bottom and at each drawpoint.

To illustrate the general procedure, we calculate the streamlines and the shape of the extracted zone for the case of two infinitely narrow apertures in the kinematic approximation. The velocity field is then the vectorial superposition of the two contributions. If the apertures are located symmetrically at positions $\mp L$ along the horizontal axis x, the vertical velocity reads

$$V = \frac{-Q}{\sqrt{4\pi D_P y}}[\mathrm{e}^{-(x-L)^2/4D_P y} + \mathrm{e}^{-(x+L)^2/4D_P y}], \tag{39}$$

where we have considered that both apertures have the same volumetric flow Q. Using Eqs. (23), the streamline equation reads

$$\frac{\mathrm{d}x}{\mathrm{d}y} = \frac{1}{2y}\left[x - L\tanh\left(\frac{xL}{2D_P y}\right)\right]. \tag{40}$$

Here, the hyperbolic tangent is clearly the interaction term due to aperture proximity. Although a full analytic solution of Eq. (40) is difficult, it can be shown that when $x \sim \pm L$, and y is small, such that the hyperbolic tangent has saturated to ± 1, the streamlines are nearly parabolic centered on each aperture. In the region of

highest interaction, i.e., $x\sim 0$ and y relatively large, ($xL/2D_P y \ll 1$), Eq. (40) becomes $\mathrm{d}x/\mathrm{d}y = (1/2y)[x - xL^2/2D_P y]$, whose solution is $Cx^2 = y\exp(L^2/2D_P y)$, where C is a constant that labels the streamlines considered. The approximated solution tells us that in the interaction region, streamlines are nearly parallel to the vertical axis. In addition, the transition from parabolas to straight lines occurs at a vertical distance given by $y_{\parallel} \simeq L^2/2D_P$.

Although the analysis above gives us a good idea of the streamline geometry, it does not provide an explicit formula for the resulting drawbody. We therefore developed a simple numerical algorithm to follow the particle trajectories and thus, retrace the wanted shape. Results are presented in Fig. 6 for several values of extracted volumes and two values of D_P. At low extracted volumes and relatively small D_P, the extracted zone is just a superposition of the two isolated drawbodies. However, as the extracted volume or D_P are both increased, the interaction region grows, producing a flow that is almost vertical in the symmetry plane between hoppers. The vertical distance for which the interaction becomes dominant is roughly given by $y_{\mathrm{int}} \simeq L^2/2D_P$. However, when a hopper has a finite size aperture, a new scale appears, and we anticipate that the interaction region dominates at vertical distances $y_{\mathrm{int}} \simeq (L-D)^2/2D_P$. Experiments performed in a two-dimensional configuration [12] show that, for the case of loose packing preparation, the superposition principle quantitatively accounts for the flows and the observed extracted zone due to two apertures. A detailed comparison of these results with more experimental findings will be presented elsewhere.

The generalization of the calculation of the extracted zone, for finite size apertures in three dimensions, is in principle direct. However, due to the complexity of the differential equations encountered,, analytical solutions remain elusive. Hence, numerical calculations should prove useful to compute drawbody shapes arising from complex configurations. We have given above the basis to perform such calculations.

5.2. Extracted zone for two apertures when alternating extractions

The main difficulty to determine the exact shape of the extracted zone, in the case of alternating extraction, is because such a zone is not just the superposition of the isolated drawbodies produced separately by each aperture. To illustrate the main features of this geometric zone, we consider only cases in which the flow is radial. Then, we begin by using the Bergmark–Roos model for the three-dimensional configuration. Without loosing generality, we locate the apertures along the y-axis, a distance L apart, at positions 0 and L, respectively (see the schema in Fig. 7). The apertures are circular of a radius $r_D \sin\theta_G$. As before, r_D is the distance from the origin of coordinates to the border of the aperture and the maximum angle for which the material is allowed to flow is θ_G. θ_0 and θ_L are the respective angles that the vectors $\overrightarrow{r_0}$ and $\overrightarrow{r_L}$ (whose origins locate at each aperture) make with respect to the vertical. As $\overrightarrow{r_0}$ and $\overrightarrow{r_L}$ describe both the same point of coordinates (x,y,z), we have, $r_0^2 = x^2 + y^2 + z^2$, $r_L^2 = x^2 + (y-L)^2 + z^2$ and $\cos\theta_0 = z/r_0$, $\cos\theta_L = z/r_L$. With these definitions, the isolated drawbodies are written as, ${}^{\mathrm{id}}r_{0,L} = r_D + (r_{\max} - r_D)(\cos\theta_{0,L} - \cos\theta_G)/(1-\cos\theta_G)$. Let us assume that the first extraction occurs at the left hopper during a time t_0,which in turn defines the volume of the isolated drawbody or equivalently its maximum height, $r_{\max}(t_0)$. Then, during a time t_0 all the particles located at ${}^{\mathrm{id}}r_0$ flow through the left aperture and the flow has influenced the position of particles initially located inside the second drawbody and its neighborhood. Therefore, the problem of determining the global extracted zone, with respect to the initial location of all fragments, reduces to calculating the initial location of the fragments that, after a time t_0, move to the boundary of the isolated drawbody

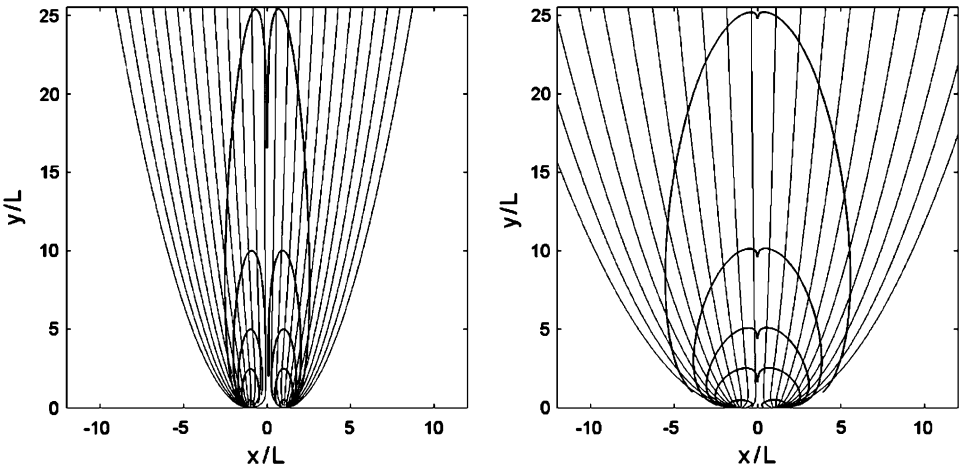

Fig. 6. Shape of the extracted zone and streamlines for different maximum heights of the draw body, $y_{\max}/L = 0.5, 2.5, 5, 10, 25.4$, with $L = 2$. Left panel, $D_P = 0.5$. Right panel $D_P = 1.0$. D_P and L are expressed in arbitrary units of length.

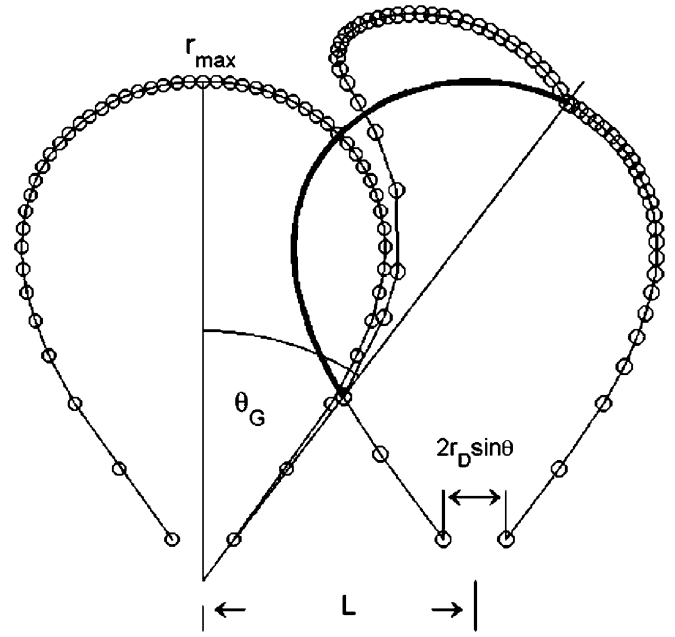

Fig. 7. The extracted zone after two alternate extractions. First, the particles are extracted from the left draw point, and then from the right one. The oblique solid line whose inclination is given by θ_G, produces a cone of revolution, centered at the origin, that indicates the interaction region. The thicker line indicates the zone of the isolated drawbody that is affected by the first extraction. The parameters are: the maximum height of the isolated extracted zone, $r_{\max} = 10$, the maximum allowed angle for displacement, $\theta_G = 35^\circ$, the radius of each aperture, $r_D \sin\theta_G = 1$, and the separation distance between orifices, $L = 5$. Distances L, r_D and $r_{\max}$ are expressed in arbitrary units of length.

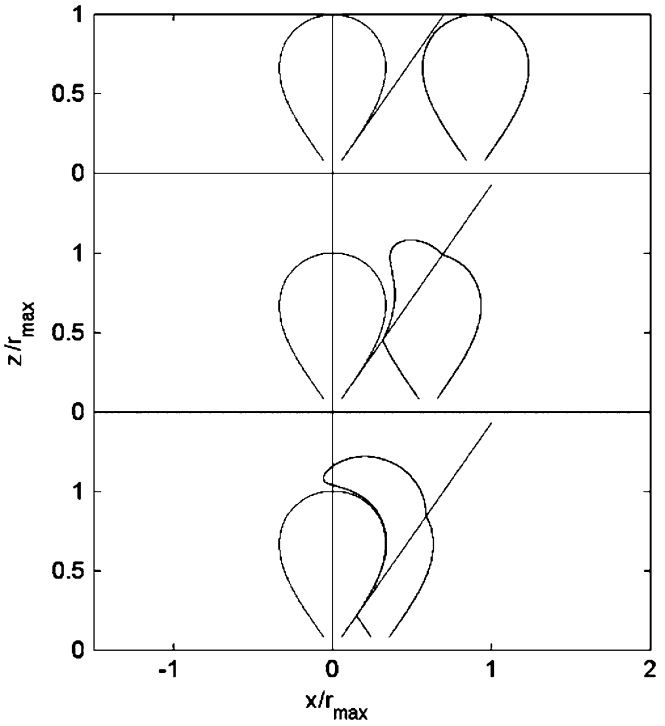

Fig. 8. The evolution of the extracted zone as decreasing the separation distance; $L = 9, 6, 3$, for $r_{\max} = 10$, $r_D = 1$ and $\theta_G = 35^\circ$. All distances are expressed in arbitrary units of length. The figures illustrate projections on the plane $[x, z]$. As in Fig. 7, oblique solid lines which have equal inclination given by θ_G, produce revolution cones, centered on 0, that indicate the interaction regions. Notice that the resulting extracted zone no longer has the revolution symmetry.

centered on $y = L$ and whose volume is defined by a extraction time t_L. Thus,

$$^{\mathrm{id}}r_{L\to 0}(t_L) = r_0(t_0) - (r_{\max}(t_0) - r_D)\frac{\cos\theta_0 - \cos\theta_G}{1 - \cos\theta_G}, \qquad (41)$$

where $^{\mathrm{id}}r_{L\to 0}(t_L)$ represents simply the form of the isolated drawbody centered on $y = L$ expressed in terms of the coordinates centered on $y = 0$. In general, the formula above has a direct geometrical interpretation that allows us to find the interaction region. Indeed, this region is basically the boundary of the drawbody with origin in $y = L$ displaced in the radial direction with respect to $y = 0$, a distance given by, $(r_{\max}(t_0) - r_D)\cos\theta_0 - \cos\theta_G/1 - \cos\theta_G$.

Calculation of the extracted zone for two drawpoints, in the case of plasticity models (for which the flow is radial as well), can be performed in a similar manner. The extracted zone in this case is given by

$$^{\mathrm{id}}r^3_{L\to 0}(t_L) = r_0^3(t_0) - 3r_D^2 V_0 t_0(\cos\theta_0 - \cos\theta_G). \qquad (42)$$

In Fig. 7, we illustrate the procedure to calculate the shape of the total extracted zone when extractions have equal volume or equivalently, $t_L = t_0$. We begin by noticing that, when $\theta_0 \geqslant \theta_G$ the boundary of the total extracted zone coincides with the corresponding isolated one since the first flow does not affect such regions. In contrast, the thicker line represents the area of the isolated drawbody that is actually affected by the first flow. Predictions from Eq. (42) are plotted in Fig. 8 for several hopper separations L. For separation distances that are slightly larger than the width of an isolated drawbody, drawbodies do not interact and the resulting extracted zone is equal to the boundary defined by the two isolated drawbodies. However, as the separation decreases, due to flow interaction, a nontrivial form for the extracted zone is observed. Thus, in this model, the drawboby interaction takes place only if some portion of the isolated drawbody, centered in L, goes into the angular section (solid line in Fig. 7) in which the first flow takes place.

6. Conclusions

In conclusion, drawbodies based on radial flows are rather insensitive to the details of the model used to predict the flow as long as the angular dependence of the flow is introduced correctly. In turn, the kinematic model is well suited for predicting the flow and, therefore, the drawbody shapes in the case of loosely packed granulates. In addition, thanks to linearity, the kinematic model holds for cases in which the extraction takes place simultaneously at several apertures. Results from these analyses should be valuable when optimizing mineral recovery in mining industry. As a general conclusion, for nonlinear flows

when simultaneous extraction is desired, a simple analysis to understand the interaction region can be performed by assuming that, in first approximation, the superposing principle holds. Thus, the sum of the velocity fields resulting from each aperture, considered as isolated, can be first assumed as a solution for the general flow. Corrections to this approximation can be evaluated by inserting the linear solution plus a disturbance into the general equation governing the flow, if it is available. This is basically the application of perturbation theory to the flow problem and will be discussed in a forthcoming publication. It is worth noting that we have not considered here hoppers of complex geometry as the ones encountered in practical applications. However, it can be stated that the variety of drawbody shapes that might arise from complex procedures, either in simultaneous or sequential extractions, can be fully characterized by the knowledge of the flow taking place at a single aperture. Realistic information on this matter can be obtained from either model experiments or in situ observations.

Acknowledgments

We are very grateful to M. Telias and V. Encinas for fruitful discussions on practical problems regularly encountered in block caving techniques. We also acknowledge E. Arancibia and the Department of Underground Mining of Chuquicamata, Codelco Norte, for partial financial support. This work had the support of IM2 under Grant IM2 No. 20/04 and Conicyt under research program Fondap No. 11980002.

References

[1] Brown ET. Block caving geomechanics. The international caving study stage I-1997 through 2000. The University of Queensland, Australia; 2003.
[2] Rustan A. Gravity flow of broken rock—what is known and unknown. In: Proceedings of MassMin 2000, Brisbane, Australia; 2000. p. 557–567.
[3] Bergmark JE. The calculation of drift spacing and ring burden for sublevel caving. LKAB Memo # RU 76-16, 1975 (in Swedish).
[4] Kuchta ME. A revised form of the Bergmark–Roos equation for describing the gravity flow of broken rock. Mineral Resources Eng 2002;11:349–60.
[5] Nedderman RM. Statics and kinematics of granular materials. Cambridge: Cambridge University Press; 1992.
[6] Mullins WW. Experimental evidence for the stochastic theory of particle flow under gravity. Powder Technol 1976;9:29–37.
[7] Litwiniszyn J. The model of a random walk of particles adopted to researches on problems of mechanics of granular. Bull Acad Pol Sci Ser Sci Technol 1963;9:61.
[8] Nedderman RM, Tüzün U. A kinematic model for the flow of granular material. Powder Technol 1979;22:243–53.
[9] Caram H, Hong DC. Random-walk approach to granular flows. Phys Rev Lett 1991;67:828–31.
[10] Samadani A, Pradham A, Kudrolli A. Size segregation of granular matter in silo discharges. Phys Rev E 1999;60:7203–9.
[11] Bransby PL, Blair-Fish PM. Initial deformations during mass flow from a bunker: observation and idealizations. Powder Technol 1975;11:273–88;
Levinson M, Shmutter B, Resnick W. Displacement and velocity fields in hoppers. Powder Technol 1977;16:29–43.
[12] Fuentes C, Apablaza V. Bi-dimensional experimentation on gravitational flow for underground Chuquicamata. Internal Report, IM2. Codelco-Chile 2003;
Melo F, Vivanco F, Fuentes C, Apablaza V. Draft report on quasi static granular flows: dilatancy effects. Internal Report IM2. Codelco-Chile 2005.